THE JOURNAL OF PHYSICAL CHEMISTRY B

Article

pubs.acs.org/JPCB

Monte Carlo Studies on the Interfacial Properties and Interfacial Structures of Ternary Symmetric Blends with Gradient Copolymers

Dachuan Sun and Hongxia Guo*

Beijing National Laboratory for Molecular Sciences, Joint Laboratory of Polymer Sciences and Materials, State Key Laboratory of Polymer Physics and Chemistry, Institute of Chemistry, Chinese Academy of Sciences, Beijing 100190, China

Supporting Information

ABSTRACT: Using Monte Carlo simulation methods, the effects of the comonomer sequence distribution on the interfacial properties (including interfacial tension, interfacial thickness, saturated interfacial area per copolymer, and bending modulus) and interfacial structures (including chain conformations and comonomer distributions of the simulated copolymers at the interfaces) of a ternary symmetric blend containing two immiscible homopolymers and one gradient copolymer are investigated. We find that copolymers with a larger composition gradient width have a broader comonomer distribution along the interface normal, and hence more pronouncedly enlarge the interfacial thickness and reduce the interfacial tension. Furthermore, the counteraction effect, which arises from the tendency of heterogeneous segments in gradient copolymers to phase separate and enter their miscible phases to reduce the local enthalpy, decreases the stretching of copolymers along the interface normal direction. As a result, copolymers with a larger width of gradient composition can occupy a larger interfacial area and form softer monolayers at saturation and are more efficient in facilitating the formation of bicontinuous microemulsions. Additionally, chain length ratio, segregation strength, and interactions between homopolymers and copolymers can alter the interfacial character of gradient copolymers. There exists a strong coupling between the comonomer sequence distribution, chain conformation, and interfacial properties. Especially, bending modulus is mainly determined by the complicated interplay of interfacial copolymer density and interfacial chain conformation.

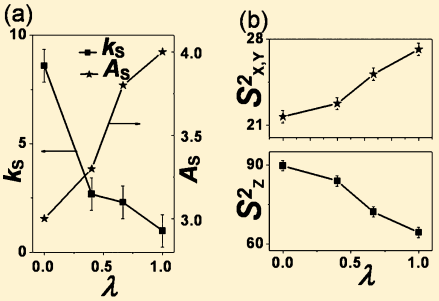

1. INTRODUCTION

Compared with synthesizing new polymers, blending currently existing polymers with desired properties to form polymer alloys is usually more cheap and recyclable, and is thus a relatively convenient route to create new useful materials. The properties of thus-formed polymer alloys could be tuned by changing the volume fraction and chemistry composition of their component materials.[1−5] However, in most cases, the miscibility between different polymer materials is low, which results in a weak interfacial adhesion and ultimately deteriorates the mechanical properties of the alloy. Thus, copolymers are often added as polymeric surfactants, helping to lower the interfacial tension (γ), stabilize the dispersed phase, and improve the interfacial mechanical strength of polymer blends.[6]

As copolymers are usually the most expensive component in polymer alloys, they are expected to achieve ultralow interfacial tension with as small amount as possible and preferentially segregate at interfaces instead of micellization in homopolymer phases. When the interfacial tension reduces to zero, the interface is taken to be saturated by copolymers and the associated interfacial area occupied by each copolymer chain at the interface is denoted as A_S. A_S can be determined using neutron reflection method in experiments.[7,8] A larger value of A_S means that fewer copolymer chains are needed to saturate the same sized interfacial area. As proposed by Sottmann et al.,[8] the efficiency of a surfactant is judged by the amount of surfactants required to reduce the interfacial tension by the same amount. This criterion could be used to evaluate copolymers. Recognition of the control parameters for A_S is helpful to choose efficient copolymers as emulsifiers.

With the sufficient addition of copolymers, the microemulsion can form, either in a droplet or a bicontinuous morphology. The bicontinuous microemulsion is thermodynamically stable and widely used to prepare interpenetrated elastomers and tunable porous membranes[9] or as templates for nanoporous materials.[10,11] Its formation, first of all, requires a vanishing interfacial tension ($\gamma \approx 0$), which could be achieved by adding sufficient amount of copolymers into the blend. Additionally, the nearby copolymer monolayers cannot have apparent attractions, which calls for a small chain length ratio between homopolymers and copolymers.[12] Moreover, the copolymer monolayers at interfaces need to be flexible with a small bending modulus (k_S). A low bending modulus means less resistance of the interface against bending or more proneness to the thermal undulations. Thus, knowledge of the key parameters governing k_S is important for better tuning the formation condition of microemulsions. k_S could be extracted using high-resolution scatter techniques in experi-

Received: February 29, 2012
Revised: July 19, 2012
Published: July 20, 2012

   dx.doi.org/10.1021/jp3020172 | J. Phys. Chem. B 2012, 116, 9512−9522

ments.[13] In simulations, it can be determined by analyzing the undulation spectrum.[14−16]

In the past decades, the interfacial properties of ternary blends using traditional diblock copolymers as compatibilizers have been widely investigated. The self-consistent mean-field theory (SCFT) results from Noolandi and Hong[17] indicate that the interfacial tension decreases to zero at a smaller copolymer volume fraction, when shorter homopolymers are used in the blend. Müller and Schick[14] found that the interfacial width increases with copolymer concentration at small and modest segregation strengths while the increase becomes unapparent at strong segregation limit. Matsen[18,19] argued that the bending modulus increases with the segregation strength. In these studies, a ternary blend (denoted as A/B/AB) with only one tunable interaction parameter χ_{AB} is chosen, in which the diblock copolymers AB are synthesized using the same monomers as homopolymers A and B. More interaction parameters (i.e., χ_{AB}, χ_{CD}, χ_{AC}, χ_{BD}, and so on) are tunable in C/D/AB blends[20−24] wherein diblock copolymers and homopolymers have different chemical constitutions. Thus, altering the chemistry composition of polymer blends enriches the possibilities to tune the properties of polymer blends. Especially, introducing attraction between homopolymers and diblock copolymers may strengthen their entanglements and improve the interfacial adhesion and the whole mechanical strength of polymer alloys.

Besides diblock copolymers, other kinds of copolymers[25−27] may also be effective compatibilizers. Recently, gradient copolymers have drawn great attention due to their great promising applications,[28,29] wherein the composition of molecules varies in a controlled fashion along the chain. The blend is denoted as A/B/G in the following, when gradient copolymers (denoted as G) are added into homopolymers A and B. Traditional diblock copolymers could be deemed as gradient copolymers with no composition gradient ($\lambda \approx 0$) in chain contours[30] while linear gradient copolymers have $\lambda \approx 1$, where the gradient parameter λ characterizes the length of the composition gradient relative to the length of the entire copolymer molecule.[31] According to the experimental results from Kim et al.,[29,32] gradient copolymers are more effective than diblock and random copolymers in stabilizing the interfaces between two immiscible homopolymers, reducing the size of the dispersed phase and inhibiting the static coalescence process. With the improvement of polymerization techniques,[33] the tuning of the length of the composition gradient may become an effective way of controlling the interfacial properties, including interfacial thickness d, interfacial tension γ, bending modulus k_S, and saturated interfacial area per copolymer chain A_S. The lower interfacial tension could stabilize the finer-sized droplets, and a broader interfacial thickness could lead to the higher interfacial mechanical strength for polymer blends. According to the theoretical results from Shull et al.,[31] d increases with λ. Experimental results[34] from Yuan et al. showed that γ is much lower when gradient copolymers are added into the water/chloroform fluid instead of the diblock copolymers with the same concentration and similar molecular weights. Using SCFT methods, Lefebvre et al. predicted that γ decreases more substantially when the linear gradient copolymers are used, compared to the diblock copolymers.[35]

Although the effect of the sequence distribution in copolymers on the interfacial tension γ and interfacial thickness d has been examined so far, its influence on other key interfacial quantities, such as k_S and A_S, has not yet been investigated, to the best of our knowledge. However, such an investigation could offer useful insight into the application of real polymer blends. The A_S value could be used to select efficient copolymers, which usually have larger A_S values and require a smaller amount to let interfaces become saturated. k_S is useful to judge the formation condition of microemulsions, which often requires a small bending modulus to keep the interfacial monolayer flexible. Although the interfacial properties of polymer alloys depend significantly on the interfacial structures, the conformations of gradient copolymers and their monomer distributions at the interfaces are rarely investigated in previous theoretical and simulation works. Such an investigation is helpful for our understanding of the interfacial efficiency of copolymers and the principles for tailoring interfacial properties from a molecular aspect. Some interfacial quantities, such as interfacial thickness and averaged interfacial area per copolymer, are directly related to the monomer distributions and conformations of gradient copolymers at the interface. Additionally, it is well recognized that the variation of chain length ratio between homopolymers and copolymers (denoted as α) offers a handle to the selection between macrophase and microphase separation for a blend of homopolymers and copolymers.[12,36] With descending α, the swelling of homopolymers to the copolymer brushes increases, which could further affect some interfacial properties and interfacial structures. Similar to diblock copolymers, the emulsification capability of gradient copolymers may be altered by the segregation strength of the blend (i.e., χ_{AB}) or reinforced by introducing the attraction between homopolymers and copolymer blocks (i.e., $\chi_{AC} < 0$ and $\chi_{BD} < 0$). Therefore, a good knowledge of the influence of the segregation strength and the enthalpic interactions between copolymers and homopolymers on the interfacial properties and structures in ternary blends with two homopolymers and a gradient copolymer may give a guide for choosing suitable comonomers in copolymer synthesis.

It is therefore very significant to investigate the influences of the comonomer sequence distribution, chain length ratio, and chemistry composition of polymer chains on the interfacial properties (including interfacial tension γ, interfacial thickness d, saturated area A_S, and bending modulus k_S) and interfacial structures (including chain conformations and comonomer distributions of the simulated copolymers at the interfaces) of a ternary symmetric blend containing two immiscible homopolymers and one copolymer. Given the distinctive features of computational convenience and efficiency, Monte Carlo simulations (MC) are used, in which the polymer blends are allowed to evolve from the totally disordered states to reach their equilibrated microstructures and more detailed information on the interfacial structures can be obtained. By comparing the interfacial properties between different copolymers at various thermodynamic and composition parameters and by investigating the relation between interfacial properties, chain conformations, and the comonomer distributions of copolymers at the interface, useful guidelines can be drawn for selecting suitable copolymers and for tuning the interfacial properties in the application of polymer blends.

2. MODEL AND METHODS

Monte Carlo simulations are carried out in a cubic box with a size of $L_X \times L_Y \times L_Z(=40)$. Periodic boundary conditions are imposed in X, Y, and Z directions. Here we only consider the behavior of symmetric ternary blends containing symmetric AB

dx.doi.org/10.1021/jp3020172 | J. Phys. Chem. B 2012, 116, 9512−9522

copolymers in two immiscible homopolymers. As shown in Figure 1a, four types of copolymers are chosen with a fixed

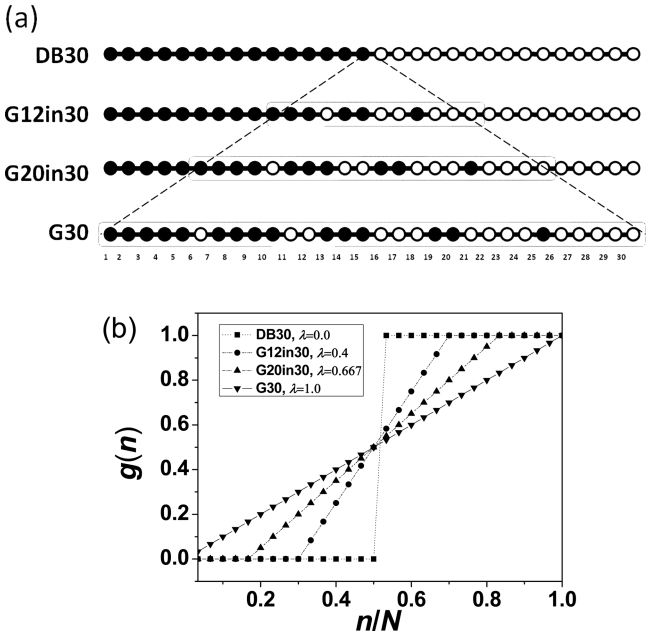

Figure 1. (a) Comonomer sequence distribution and their nomenclatures of linear copolymers. White and black beads represent segments A and B, respectively. From top down, the length of the gradient part increases and the λ values are 0, 0.4, 0.667, and 1, respectively. (b) Composition profile $g(n)$ along the normalized length n/N of the chain for the four copolymers.

length of 30. Besides, the two homopolymers are selected to have the same chain length and the same volume fraction. If the chemical compositions of homopolymers are the same with copolymers, the two homopolymers are denoted as A and B, and correspondingly the ternary blend is abbreviated to A/B/AB blend. If the chemical compositions of homopolymers are different from copolymers, they are denoted by C and D, and the corresponding ternary blend is abbreviated to C/D/AB blend. To accelerate the relaxation of chain conformations, 7% permanent vacancies (denoted V) exist in a simulation box. Permanent vacancies can be deemed as neutral solvents or free spaces.

Polymer chains in our lattice model are formed by linearly connected segments. A polymer chain with N segments is connected by $N - 1$ bonds, and the bond length ranges from 1 to $\sqrt{3}$ in the unit of lattice. Each segment occupies one lattice site and obeys the excluded volume criterion. Furthermore, the bond crossing is always forbidden. To study the effect of composition gradient, four copolymers with different sequence distributions are investigated in-depth in the following. Among them, one is a diblock copolymer (denoted as DB30), which is formed by a sequence of one block of type A segments followed by the other block of type B segments and is typically illustrated in Figure 1a. As explained earlier, the architecture of this copolymer chain corresponds to a gradient copolymer with the steplike distribution function and $\lambda = 0$. The remaining three copolymers are typical symmetric gradient copolymers consisting of equal amount of A and B segments with different lengths of linear composition gradient along the chains. Recently, Jiang et al.[37] have developed a multiblock model to study the phase behavior of gradient copolymers. Each gradient copolymer is divided into many subchains, and each subchain is assumed to be an A/B diblock copolymer whose block composition is determined by the gradient copolymer composition profile. The validity of the multiblock model of gradient copolymers is established due to the good agreement between random phase approximation results for a continuous composition distribution and a multiblock model. In our simulations, we also use the multiblock model to form the linear gradient copolymers. As illustrated in Figure 1a, G30 contains five parts of short copolymers, each with six segments, wherein the composition distribution for each part changes linearly along the entire chain. As a result, its gradient parameter is $\lambda = 1.0$. The other two gradient copolymers can be deemed as triblock copolymers, since a midblock with linear gradient composition[33] is linked to two portions of pure A and B monomers at the two ends of each copolymer chain. As the lengths of the midblock are 12 and 20, respectively, we denote them as G12in30 and G20in30. Their gradient parameters are 0.4 and 0.667, respectively, as shown in Figure 1b.

In the present work, we only consider the pairwise nearest-neighbor interaction ε. A positive value of ε means a repulsive interaction, and a negative ε value implies an attractive interaction. As just mentioned, in A/B/AB blends, copolymers AB are composed of the same monomers as homopolymers. For simplicity, only the interaction between A and B segments (denoted as ε_{AB}) is considered while all other interactions are set to be zero. Thus, it has $\varepsilon_{AB} > 0$ and $\varepsilon_{AA} = \varepsilon_{BB} = \varepsilon_{VV} = \varepsilon_{AV} = \varepsilon_{BV} = 0$. In C/D/AB blends, besides ε_{AB}, interactions between blocks A and homopolymers C as well as between blocks B and homopolymers D are also considered, in order to investigate the effect of enthalpic interactions between homopolymers and copolymers on the interfacial properties. We set $\varepsilon_{AC} = \varepsilon_{BD}$ and $\varepsilon_{AB} = 1.0$. Thus, only the interaction parameter ε_{BD} is tunable in C/D/AB blends. ε_{BD} can be positive or negative, which represents repulsion and attraction respectively.

All simulations are started by equilibrating the systems in the athermal limit, i.e., $\varepsilon_{AB} = 0$ (and $\varepsilon_{BD} = 0$). Then, those totally disordered configurations are quenched to any required values of ε_{AB} (and ε_{BD}) and equilibrated again. The evolution of the chain configuration is achieved by vacancy diffusion algorithm, wherein vacancy sites are selected first and tried to be exchanged with a neighbor polymer segment. Two kinds of moves, "partial reptation"[38,39] and "identity switch",[40] are also included to accelerate the simulation process. The first move is used to relax all polymer configurations and the second is used to accelerate the unmixing process of homopolymers. One Monte Carlo step (MCS) is defined as the time necessary for every segment to attempt to move once on average. After one MCS of partial reptation, an attempted identity switch is executed. Different frequencies were also attempted and the results are insensitive to the specific choice. The "switch" procedure is done by picking a homopolymer chain at random and attempting to replace it with a chain of the opposite type with its configuration unchanged. In A/B/AB blends, it means A → B or B → A exchanges, while in C/D/AB blends it has C → D and D → C switches. The chemical potential between binary homopolymers is set to be zero. Thus, the averaged volume fraction of A and B homopolymers equals with each other. Every attempted move should satisfy the excluded volume condition, the bond length restriction, and no bond-crossing criterion and is further judged by the Metropolis Rule.[41] That means, the Boltzmann factor $\exp(-\Delta E/k_BT)$ should be greater than or equal to a random number uniformly

dx.doi.org/10.1021/jp3020172 | J. Phys. Chem. B 2012, 116, 9512−9522

distributed in the interval (0,1) where ΔE is the change of energy due to this attempted move, k_B is the Boltzmann constant, and $k_BT = 1$.

At each state point, we monitor the evolution of the average energy per monomer[30] (E_m) and the structural (structure factors and density profiles) and conformational (mean-squared radius of gyration R_g^2 and mean-squared end-to-end distance $\langle S^2 \rangle$) properties of the system. The equilibration is considered to be reached when those quantities do not change with the simulation time. Starting from totally disordered states, generally at least 10^7 MCS are required to equilibrate the system and another 10^7 MCS are used to collect the data. Due to the periodic boundary condition, two flat and discrete interfaces are formed in a cubic box.[42] The two interfaces behave equivalently. After equilibrium states are reached, several interfacial and structural quantities are analyzed.

In lattice models, we can estimate γ from the spectral intensities of undulating modes if the interfacial monolayer is not highly curved. In this work, Z axis is chosen as the interface normal direction. The height fluctuation in the monolayer ($h(x,y)$) is defined as the displacement of local position ($z(x,y)$) from the average position of the interface. Here $z(x,y)$ is taken to be the location of the midpoint of each copolymer chain. According to the equipartition theorem, for small wave vectors q we can relate these undulation modes to the interfacial tension γ and the bending modulus[43,44] k

$$\langle |h(q)|^2 \rangle = k_BT(\gamma q^2 + kq^4)^{-1}/(L_X \times L_Y) \quad (1)$$

where $L_X \times L_Y$ is the area of the simulation box. From simulations we can obtain spectral intensities of undulatory modes $S(q) = \langle |h(q)|^2 \rangle (L_X \times L_Y)$. Therefore, the interfacial tension γ is obtained by fitting the plot $1/(q^2S(q)) \sim q^2$ using the equation[16,45] $y = \gamma + kx$.

When γ decreases to near-zero, interfaces between homopolymer phases are considered to be saturated by copolymers. The minimum volume fraction of copolymers to achieve $\gamma = 0$ is denoted as ϕ_S in the following. Correspondingly, the bending modulus and averaged interfacial area occupied by each copolymer chain are denoted as k_S and A_S, respectively. The number of copolymer chains locating at interface (denoted as m) can be calculated by the excess volume fraction of copolymers[46,47] in the interfacial region (denoted as ϕ_1)

$$m = (L_X \times L_Y \times L_Z \times \phi_1)/N \quad (2)$$

where N is chain length of copolymers. After we know m at $\gamma = 0$, A_S is given by

$$A_S = (L_X \times L_Y \times 2)/m \quad (3)$$

The interfacial thickness is defined as[4,48,49]

$$d = \frac{\rho_{max} - \rho_{min}}{|\nabla \rho|_{max}} \quad (4)$$

where ρ_{max} and ρ_{min} is the maximum and minimum value of the number density ρ of segments A in A/B/AB blends (or segments C in C/D/AB blends) near the interface. $|\nabla \rho|_{max}$ is the maximum slope of the density profile for that kind of segments. As the interfacial density profile can be well fitted by the tanh function,[31] the maximum slope of the density profile curve is usually estimated from the middle of the interface. Similar to the spectral method for deriving γ and k values, the method to calculate the interfacial thickness here requires that the interfaces are not highly curved and the interface normal direction remains parallel to the Z axis.

To acquire conformational information of copolymer chains at interfaces, two variables are monitored. One is the mean-squared end-to-end distance[50]

$$\langle S^2 \rangle = \frac{1}{m} \sum_{i=1}^{m} (r_N^i - r_1^i)^2 \quad (5)$$

where m is the number of copolymers enriched at the interfaces. r_N^i and r_1^i are coordinates of chain ends for the ith copolymer. To reflect the variations of copolymer conformations along the X, Y, and Z directions, the three components of S_X^2, S_Y^2, and S_Z^2 are also measured along coordinate axes. $S_{XY}^2 = {}^1/_2(S_X^2 + S_Y^2)$ is the arithmetic average of two components of the mean-squared end-to-end distance $\langle S^2 \rangle$ in the plane parallel to the interface. The other is the radius of gyration[50]

$$R_g = \left[\frac{1}{mN} \sum_{i=1}^{m} \sum_{j=1}^{N} (r_j^i - R_{C.M.}^i)^2 \right]^{1/2} \quad (6)$$

when $R_{C.M.}^i$ is coordinate of center of mass of the ith copolymer.

In our MC simulations, the sequence distributions of copolymers and interactions between segments of different kind could be controlled at will and the resulting microstructures can be examined in all detail.[51] In the following, we examine the interfacial tension, interfacial thickness, and copolymer conformations from low copolymer concentrations up to the saturation limit, and the chain length ratio between homopolymers and copolymers (α) is changed by varying the homopolymer length N_H from 2 to 30 while fixing copolymer length N_C at 30. The segregation strength ε_{AB} is changed from 0.2 to 1.0 for A/B/AB blends and the interaction $\varepsilon_{BD}(=\varepsilon_{AC})$ between homopolymer segments and corresponding copolymer blocks in the C/D/AB blends varies in the range of −0.3 to 0.2. Under these conditions, these blends are all in the macrophase-separated (2P) state, wherein the copolymers form two discrete monolayers at the interfaces between two immiscible homopolymer phases.

3. RESULTS AND DISCUSSION

3.1. Effect of Compositional Gradients. First, we consider the effect of compositional gradients on the interfacial properties, i.e., interfacial tension, interfacial thickness, bending modulus, and the projection area per copolymer chain, as well as on the interfacial structures, including the comonomer distributions and conformational properties of interfacial copolymers.

3.1.1. Interfacial Tension and Interfacial Thickness. Figure 2, a and b, shows the variation of interfacial tension γ and interfacial thickness d with copolymer volume fraction ϕ_C for different gradient parameter λ in typical A/B/AB blends with $\varepsilon_{AB} = 1.0$ and $\alpha = 1.0$. For diblock copolymers with $\lambda = 0.0$, γ decreases with ϕ_C in Figure 2a, consistent with previous theoretical[52] and experimental[53,54] results. For a given ϕ_C, γ decreases with λ in Figures 2a, which is also in agreement with previous theoretical results[35] from Lefebvre et al. When γ decreases to zero, we get the saturated concentration ϕ_S. Noting that in Figure 2b, d is plotted against ϕ_C until ϕ_S. In contrast to the change of γ, with increasing λ the value of d increases. The decrease of γ and the increase of d with increasing λ are observed in other A/B/AB blends, such as at α

dx.doi.org/10.1021/jp3020172 | J. Phys. Chem. B 2012, 116, 9512−9522

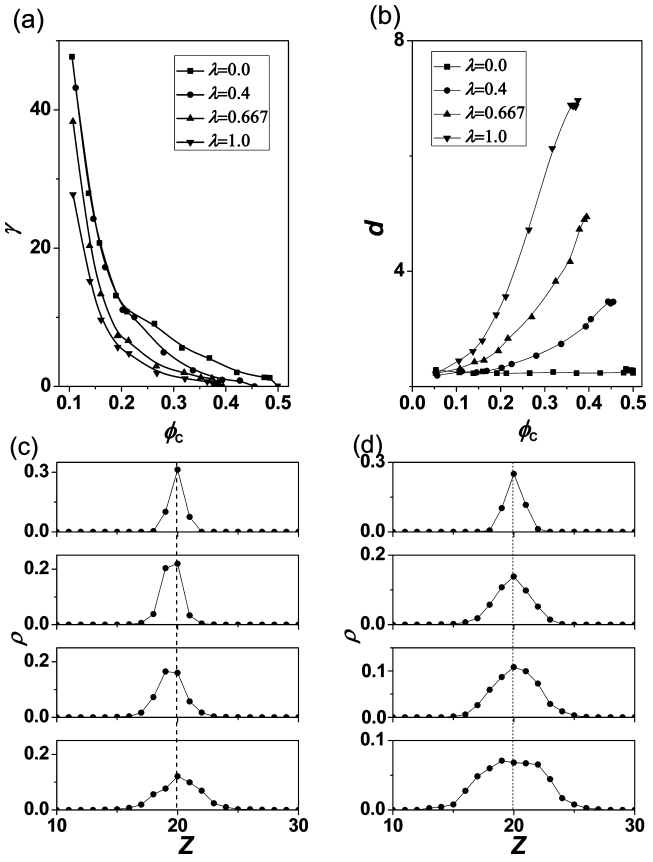

Figure 2. (a) Interfacial tension γ and (b) interfacial thickness d as a function of the copolymer volume fraction ϕ_C in A/B/AB blends at chain length ratio α = 1.0 and segregation strength ε_{AB} = 1.0. Normalized density profiles for the joint-point segments for copolymers with different λ values at (c) ϕ_C = 0.25 and (d) ϕ_C = ϕ_S, respectively. For clarity, only one monolayer is shown and the dashed line shows the location of interface (at position Z = 20). The λ values are 0, 0.4, 0.667, and 1, respectively, from the top to the bottom in panels (c) and (d).

= 0.2 and ε_{AB} = 0.5. As the critical interaction ε_{AB} for the demixing transition in A30 + B30 binary blends is at ε_{AB} = 0.02, the ternary blends containing diblock copolymers (i.e., λ = 0.0) at ε_{AB} = 1.0 are expected to be in the strong segregation regime. Both SCFT[46] and MC simulations[14] indicate that d increases with the diblock copolymer content at weak and intermediate segregation strengths. Results from Müller and Schick[14] indicate that the increase of d becomes negligible at strong segregation regime. Consistent with their results, the d value in Figure 2b for A/B/AB blends at λ = 0.0 shows no apparent variations with ϕ_C while it increases significantly at λ > 0.0.

The growth of d with λ can be attributed to the spatial distribution of copolymer comonomers at the interface. Along the copolymer chain contour, there exist several segments with the species type different from at least one of their nearest neighbors. We call them as *joint-point segments* in the following. As shown in Figure 1, the number of joint-point segments increases with λ. At λ = 0.0, these joint-point segments are at the center of each copolymer chain while they distribute to the whole chain when λ increases to 1.0. Panels c and d of Figure 2 are the number density profiles for those joint-point segments at typical copolymer volume fractions of ϕ_C = 0.25 and ϕ_C = ϕ_S, respectively, where ϕ_S is the saturated volume fraction of copolymers. Apparently, the cumulant value increases with ϕ_C for all λ values. At small ϕ_C those joint-point segments are mostly located within a small interface region, while at higher ϕ_C their distribution becomes wider along the interface normal direction for copolymers with λ > 0.0. In Figure 2c, at the same volume fraction of copolymers (i.e., ϕ_C = 0.25), the distribution of joint-point segments are much wider along the interface normal direction for copolymers with bigger λ values, in line with SCFT results from Wang et al.[55] More interestingly, a detailed comparison between panels c and d of Figure 2 indicates that the width of the density distribution of joint-point segments nearly does not change for diblock copolymers (i.e., λ = 0.0), although the copolymer volume fraction is increased from 0.25 to ϕ_S = 0.50. This phenomenon, together with the invariance of d with ϕ_C at high segregation strength ε_{AB} for λ = 0.0, indicates that the comonomers in individual diblock copolymers are well separated at the interface at the high segregation strength. In contrast, we find that the density distribution of joint-point segments broadens as ϕ_C is increased for λ > 0.0. Therefore, with increasing λ or ϕ_C or both, the broader distribution of joint-point segments brings a wider interfacial region between two homopolymer phases and thus the interfacial thickness d is increased with λ and ϕ_C for λ > 0.0 in Figure 2b.

3.1.2. Copolymer Conformations at the Interface. With increasing copolymer volume fraction ϕ_C, the packing of copolymers at interfaces becomes more crowded. Accompanied with the decrease of the interfacial tension γ and the increase of the interfacial thickness d, these copolymers are expected to stretch along the interface normal direction. In Figure 3a, we plot the components of the mean-squared end-to-end distance $\langle S^2 \rangle$ with the reduced volume fraction (ϕ_C/ϕ_S), which is defined as the ratio of the volume fraction of copolymers ϕ_C to their saturated concentration ϕ_S. In this way, the comparison of the parallel and perpendicular components of $\langle S^2 \rangle$ (i.e., S_{XY}^2 and S_Z^2) can be made at the same saturation content. As expected, the conformations of copolymers are compressed in the plane parallel to the interface and both S_X^2 and S_Y^2 decrease with increasing ϕ_C. Meanwhile, copolymer chains are stretched along the interface normal direction and S_Z^2 increases with ϕ_C, as shown in Figure 3a. Furthermore, at the same content of saturation (ϕ_C/ϕ_S), S_Z^2 decreases with λ while both S_X^2 and S_Y^2 increase with λ.

Although we just illustrated that the distribution of the joint-point segments along the copolymer chains drives the growth of the interfacial width with λ, to explain the change of chain conformations with gradient parameter λ, we need to further investigate the distribution for each segment of copolymers along the interface normal direction. We note that, for a gradient copolymer chain with λ > 0, in each half-chain, there are several segments with the species type different from the majority segments. We call these minorities as *heterogeneous segments* in the following. For example, as illustrated in Figure 1a, in each G30 chain, the 6, 11, and 12 are B segments embedded in the left half-chain rich in A segments, while the 19, 20, and 25 segments are also of different kind with the majority segments in the right half-chain. Therefore, each G30 chain has six heterogeneous segments in our model. We find that the counteraction effect, which arises from the tendency of heterogeneous segments in gradient copolymers to phase separate and enter their miscible homopolymer phases to reduce the local enthalpy, reduces the stretching of copolymers along the interface normal direction.

dx.doi.org/10.1021/jp3020172 | J. Phys. Chem. B 2012, 116, 9512−9522

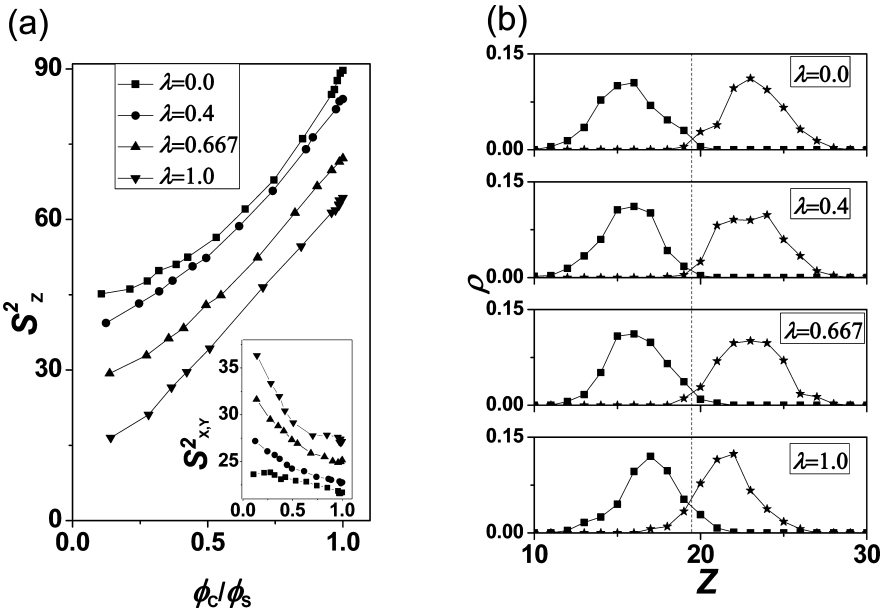

Figure 3. (a) Component of the mean-squared end-to-end distance $\langle S^2 \rangle$ along the interface normal direction as a function of the copolymer volume fraction ϕ_C normalized by their respective saturated volume fraction ϕ_S; the inset shows the component of $\langle S^2 \rangle$ for interfacial copolymers along the plane parallel to the interface. (b) Density profiles along the interfacial normal direction for the sixth (square) and 25th (star) segments (see Figure 1a) in four copolymers with different λ values at $\phi_C = \phi_S$. All data are derived at the condition of $\alpha = 1.0$, $\varepsilon_{AB} = 1.0$.

Taking the 6th and 25th segments in G30 as an example, we draw the profiles of their number density distributions in Figure 3b. For comparison, the distribution profiles for the 6th and 25th segments in DB30, G12in30, and G20in30 are also shown in Figure 3b. Note that for the copolymer chains with $0 \leq \lambda < 1$, the 6th and 25th segments are of the same kind with their neighboring segments; while in G30, the 6th and 25th segments are A and B segments respectively and of different kind from their neighbors, as shown in Figure 1a. Despite this apparent discrepancy, these segments are at the same distance (about 10 lattice size) to the chain center. We should point out that, in Figure 3b, the left and right regions stand for the phases of homopolymer B and A, respectively, although their density profiles are not shown for clarity. We see that the heterogeneous segments in G30 move toward the interface and attempt to enter their favorable domains. In contrast, the 6th and 25th segments in the diblock copolymer (DB30) are well separated with a very small overlap between their densities. Additionally, for the 6th and 25th segments in G12in30 and G20in30 copolymers, the peak positions of the density profiles move close to the interface and the overlap is enhanced compared with DB30, as shown in Figure 3b. We speculate that, although the 6th and 25th segments are not heterogeneous segments in G12in30 and G20in30 copolymers, the counteraction effect from the heterogeneous segments within the "mid-block" of these copolymers drives them toward the interface. As the length of such "mid-block" shortens with decreasing the gradient width λ, the counteraction effect weakens. Thus, the peak position moves closer to the interface and the density overlap between the 6th and 25th segments near the interface increases from top to bottom in Figure 3b with increasing λ.

It is clear that the copolymers with larger λ have a broader comonomer distribution along the interface normal, which drastically displaces the immiscible homopolymers from the interface, and hence more pronouncedly enlarges the interfacial thickness and more substantially reduces the interfacial tension. Furthermore, the local segregation of the heterogeneous segments induces counteraction or withdrawing forces to each half-chain, and eventually the copolymers with larger λ take on less stretching conformation in the direction perpendicular to the interface. Apparently, the spatial distribution of copolymer monomers is crucial for understanding the interfacial properties, such as γ and d, and chain conformations. Such microscopic details are difficult to access by experimental studies.

3.1.3. Bending Modulus and Saturated Area for Copolymers at the Interface. Despite considerable work[31,34,35] on the influence of composition gradient on the interfacial thickness d and interfacial tension γ, the influence of composition gradient on the saturated interfacial area A_S per copolymer and the saturated bending modulus k_S, as well as their relation with the conformational properties of interfacial copolymers, is still relatively unclear. Such knowledge is of great utility in rational selection and design of the comonomer sequence distributions to facilitate the formation of bicontinuous microemulsions. As defined before, the interfaces are considered to be saturated when γ approaches zero, and the corresponding bending modulus k and projection area A are denoted as k_S and A_S, respectively. Previous investigations indicate that the bending modulus is proportional to the chain length but in reverse proportion to the area per molecule at saturation states.[56,57] As the copolymer with a larger λ value has an expanded conformation in the plane parallel to the interface but a compressed conformation along the interface normal direction, it is expected to take more area on the interface and stretch to a less extent in the direction perpendicular to the interface. We hence infer that the bending modulus is decreased with λ. Figure 4a indeed shows that A_S increases with λ and k_S decreases with λ, suggesting that copolymers with a larger width of gradient composition can occupy a larger interfacial area than traditional diblock copolymers and form softer monolayers at saturation. Thus, copolymers with a

dx.doi.org/10.1021/jp3020172 | J. Phys. Chem. B 2012, 116, 9512−9522

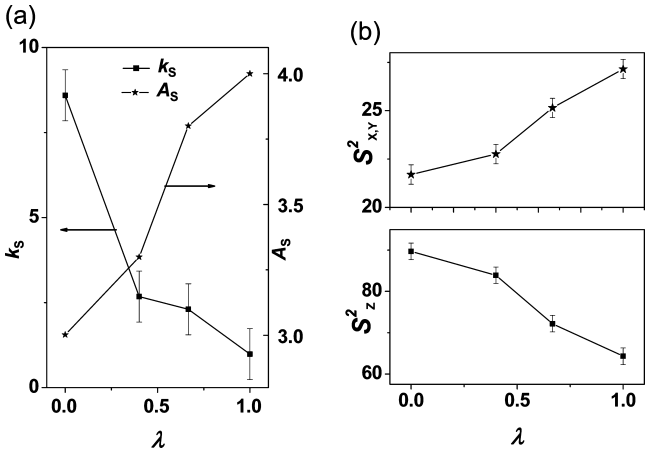

Figure 4. (a) Bending modulus k_S and averaged interfacial area per copolymer chain A_S, and (b) the components of the mean-squared end-to-end distance as a function of λ at $\phi_C = \phi_S$, $\alpha = 1.0$, and $\varepsilon_{AB} = 1.0$. The error bar is given for k_S while the statistical error is smaller than the label size for A_S values.

gradient in composition facilitate the formation of microemulsions.

In order to have an insight into the role of copolymer conformation in dictating A_S and k_S, we summarize the changes of S_Z^2 and S_{XY}^2 for the interfacial copolymers at saturation states in Figure 4b. We see that the growth of S_{XY}^2 with λ is well keeping with the increase of A_S with λ. The lowering of S_Z^2 with λ is consistent with the reducing of k_S with λ. These observations supported the proposition that the chain conformations have a direct influence on the interfacial properties. A_S is insensitive to the box size L.[58] For example, for the A30 + B30 + DB30 blends at $\varepsilon_{AB} = 1.0$ and $\gamma = 0$, A_S is calculated to be 3.0 ± 0.05, 3.0 ± 0.05, and 3.1 ± 0.05, as L increases from 40 to 60 then to 80, respectively. The corresponding bending modulus values are 8.6 ± 1.0, 8.8 ± 1.0, and 7.7 ± 1.0, respectively, which are close to each other within error bars. The system size $L = 40$ is a suitable box size to determine the bending modulus, because it is larger than the interfacial thickness (in Figure 2b, $d = 6.9$ for the ternary blends A30 + B30 + G30 at segregation strength $\varepsilon_{AB} = 1.0$ and $\phi_S = 0.37$) and also larger than the crossover wavelength of 6.0 (the ln $S(q) \sim$ ln q plots indicate that the crossover occurs at a wavevector of approximately $q = 1.0$).

As demonstrated above, due to the counteraction effect, for the copolymers at the saturated interface, the stretching along the interface normal direction decreases while the expanding in the plane parallel to the interface increases with λ. As a result, high S_{XY}^2 arising from large λ yields the relatively strong lateral repulsions between copolymers, such that the near-zero interfacial tension is achieved with small A_S. High S_Z^2 resulting from low λ yields a high degree of orientation ordering and such an stretched molecule equals with a chain with larger molecular weight, and thus enhances the rigidity against bending deformations for the interfacial molecules.[59] On the basis of these simulation studies, we can see that the interfacial properties such as A_S and k_S depend significantly on the comonomer sequence distribution of the individual copolymer and chain conformation.

3.2. Other Factors That Influence the Interfacial Properties and Copolymer Conformations. Besides λ, the interfacial properties could be influenced by the blend composition and thermodynamic parameters. To better understand the interfacial behavior of gradient copolymers, we have studied the effect of homopolymer chain length N_H (or the ratio α between the lengths of homopolymers and copolymer chains), segregation strength ε_{AB}, and interactions between homopolymers and copolymers ε_{BD} (in C/D/AB blends) on the interfacial properties and the interfacial structures. In the following, all these properties will be calculated under condition $\gamma = 0$. In this way, we can compare the interfacial quantities, such as k_S and A_S in the same saturated states, resembling part of the saturated monolayer with vanishing interfacial tension in microemulsions.

3.2.1. Effect of Chain Length Ratio α. Consistent with Noolandi and Hong et al.,[17] we found that the interfaces reach saturation at smaller volume fractions of copolymers and thus the averaged saturated interfacial area per copolymer A_S becomes bigger when shorter homopolymers are used. As shown in Figure 5a, A_S increases with decreasing α (or N_H, as the copolymer length herein is fixed at 30). Compared with long homopolymers, shorter homopolymers lose less conformational entropy when they are trapped within the copolymer monolayers, and they are more capable to swell the copolymer brushes. This swelling enlarges the averaged distance between neighboring copolymer chains and expands

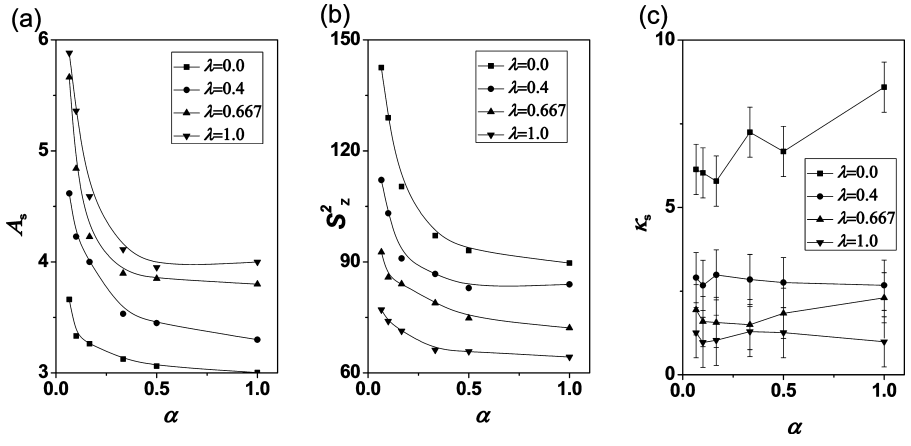

Figure 5. (a) Saturated area per copolymer A_S, (b) the perpendicular component of the mean-squared end-to-end distance S_Z^2, and (c) bending modulus k_S as a function of the chain length ratio between homopolymers and copolymers α at $\varepsilon_{AB} = 1.0$ for A/B/AB blends.

dx.doi.org/10.1021/jp3020172 | J. Phys. Chem. B 2012, 116, 9512−9522

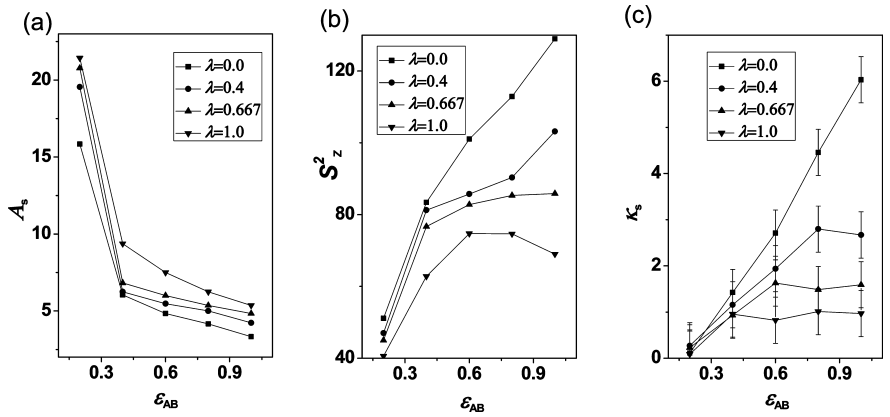

Figure 6. (a) A_S, (b) S_Z^2, and (c) k_S as a function of the segregation strength ε_{AB} at α = 0.1 for A/B/AB blends with different λ values.

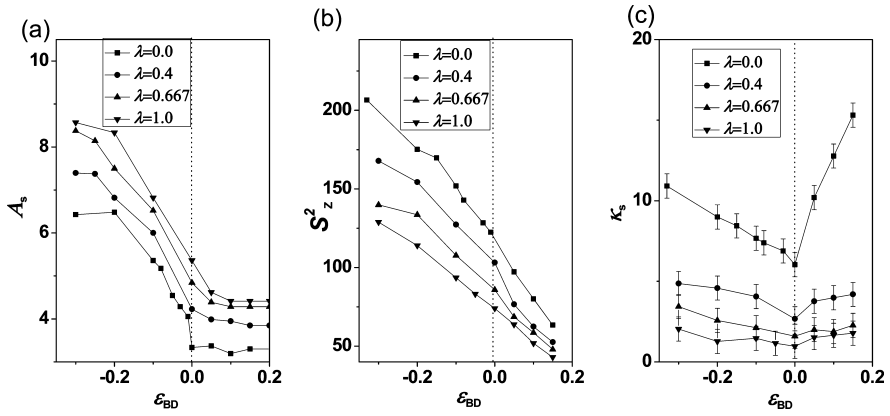

Figure 7. For C/D/AB blends at α = 0.1 and ε_{AB} = 1.0, (a) A_S, (b) S_Z^2, and (c) k_S as a function of the enthalpic interaction ($\varepsilon_{BD} \equiv \varepsilon_{AC}$) between homopolymers and corresponding copolymers.

the averaged projection area per copolymer. Furthermore, when copolymer monolayers are swollen by short homopolymers, the stretching of copolymer conformations along the interface normal is also enhanced, as shown by the S_Z^2 values in Figure 5b. Due to the counteraction effect, A_S increases with λ and S_Z^2 decreases with λ, at a fixed α value.

In line with SCFT results from Matesen,[60] k_S has no monotone trend of increasing or decreasing with the variations of α in Figure 5c. On the one hand, the A_S increases with descending α in Figure 5a, which means that fewer copolymers are allocated at the same interfacial area and a smaller amount of copolymer chains contribute to the bending rigidity of interfacial monolayers. Thus, the growth of A_S with decreasing α give a decreasing trend of k_S with α. On the other hand, the stretching of copolymers is also enhanced by shortening the homopolymer length N_H (or α, as $N \equiv 30$), which implies an increasing difficulty to bend monolayers composed of such stretched chains. Clearly, a complicated interplay of interfacial copolymer density and interfacial chain conformation leads to the unobvious variations of k_S with α in Figure 5c. Moreover, Figure 5c demonstrates again that k_S at large λ values is always lower than that at smaller λ values.

3.2.2. Effect of Segregation Strength ε_{AB}. To illustrate the effect of ε_{AB}, we present the results for a typical system composed of A3 + B3 + AB30 with α fixed at 0.1. As shown in Figure 6a, A_S decreases with ε_{AB} at fixed λ values. It should be noted that the unmixing point for the binary homopolymer blend A3 + B3 is ε_C = 0.17. With increasing segregation strength ε_{AB} at $\varepsilon_{AB} > \varepsilon_C$, the copolymer tends to stretch its blocks into the corresponding homopolymer phases to reduce its own enthalpy as well as those of the homopolymers it displaces from the interface. More copolymer chains are needed to saturate the same interfacial area, which causes the average projection area A_S to decrease with ε_{AB}. This trend in ternary polymer blends is very similar to the theoretical results from Rosen,[61] wherein the minimum area per surfactant increases with increasing temperature, by noting that the ε_{AB} varies reversely with the temperature T in the MC method.

Meanwhile, as shown in Figure 6b, the stretching of copolymers increases with ε_{AB} at small λ values but gradually approaches the asymptotic values for the copolymers with large λ values. This may result from the enhanced "counteraction effect" of heterogeneous segments in gradient copolymers at higher segregation strength, which more drastically withdraws the stretching of copolymers along the interface normal direction. With increasing ε_{AB}, these heterogeneous segments are more favorable to insert into their miscible homopolymer domain to reduce the greater enthalpy at higher segregation strength.

Matsen[18,19,60] argued that the bending modulus increases with the segregation strength χN in A/B/DB blends. In Figure 6c, the bending modulus k_S indeed increases with ε_{AB} for A/B/DB blends. For A/B/G blends, it first increases and then levels off with ε_{AB} at higher segregation strengths. With increasing ε_{AB}, the stretching of copolymers implies the improving rigidity for interfacial copolymers. The decease of A_S means that more and more copolymers are densely packed within the same interfacial area at higher segregation strength. Thus, both the

dx.doi.org/10.1021/jp3020172 | J. Phys. Chem. B 2012, 116, 9512−9522

mean-squared end-to-end distance S_Z^2 and the saturated area A_S give a consistent ascending trend of bending modulus k_S with increasing segregation strength ε_{AB}. For the copolymers with big λ values, the invariance of k_S with increasing ε_{AB} at higher segregation strengths can also be explained by the "counteraction effect" of gradient copolymers, which is enhanced at high ε_{AB} values. This effect causes more disruption to the stretching of copolymers, which balances with the increased interfacial density and results in the invariance of k_S at high ε_{AB} values.

3.2.3. Effect of Interactions ε_{BD} between Copolymer and Homopolymer Segments. Compared with the traditional A/B/AB blends, the relation between the enthalpic interactions and the interfacial properties of C/D/AB blends[20,62] is rarely investigated. For simplicity, we set $\varepsilon_{BD} = \varepsilon_{AC}$ and $\varepsilon_{AB} = \varepsilon_{CD} = 1.0$. Thus, only one interaction parameter ε_{BD} can be tuned in the C/D/AB blends. As illustrated in Figure 7a, A_S increases with $|\varepsilon_{BD}|$ at $\varepsilon_{BD} < 0$ and decreases with $|\varepsilon_{BD}|$ at $\varepsilon_{BD} > 0$. Moreover, the variation of A_S becomes smaller at high $|\varepsilon_{BD}|$ values. For a fixed repulsion between immiscible components, introduction of favorable interactions between homopolymer segments and copolymer blocks drives more homopolymers penetrating into the copolymer brushes and thus increases surface pressure. Thus, fewer copolymers are required to saturate a given interfacial area. In contrast, the introduction of unfavorable interactions between homopolymers and copolymers enhances the tendency of copolymer blocks to be surrounded by themselves rather than by homopolymers and lowers the effective lateral repulsion. Thus, more copolymers are needed to saturate the interface. Note that increasing the ε_{BD} repulsion to $\varepsilon_{BD} > 0.35$ brings the macrophase separation between copolymers and homopolymers in C3/D3/G30 blends, wherein part of the interface has no copolymers covered, similar to the experimental results from Chun et al.[62] Also note that, at very low ε_{BD} ($\varepsilon_{BD} < -0.4$) values, more copolymers are solubilized in homopolymer phases and few copolymers could diffuse to the interfacial region from homopolymer bulk phases. Thus, we focus on the situations at $-0.3 < \varepsilon_{BD} < 0.2$. Compared with Figure 5a, Figure 7a indicates that the improvement of A_S value could be achieved by introducing the attraction between homopolymers and copolymers without sacrificing the homopolymer lengths.

Furthermore, to maximize the favorable contacts, the attractions between homopolymers and favorable blocks enhance the stretching of interfacial copolymers, as shown in Figure 7b. Contrarily, to minimize the unfavorable contacts (the BD and AC contact pairs) at $\varepsilon_{BD} > 0$, the conformation of copolymers is more confined in the interface normal direction, as indicated by the small S_Z^2 values in Figure 7b. At $\varepsilon_{BD} < 0$, the increase of A_S gradually slows down whereas S_Z^2 still increases apparently with $|\varepsilon_{BD}|$, which means a more significant stretching of copolymers at interfaces and implies more difficulty to bend monolayers with such stretched copolymer chains. Thus, k_S has an ascending trend with $|\varepsilon_{BD}|$ at $\varepsilon_{BD} < 0$. At $\varepsilon_{BD} > 0$, the decrease of A_S with $|\varepsilon_{BD}|$ gradually slows down while S_Z^2 decreases dramatically. Thus, the increase of k_S with ε_{BD} at $\varepsilon_{BD} > 0$ may arise from the excluded volume effect, as all interfacial copolymers collapse down to the interface.

4. CONCLUSION

Monte Carlo simulation methods are used to investigate the effects of the comonomer sequence distribution on the interfacial properties (including interfacial tension, interfacial thickness, saturated interfacial area per copolymer, and bending modulus) and the interfacial structures (including chain conformations and comonomer distributions of the simulated copolymers at the interfaces) of a ternary symmetric blend containing two immiscible homopolymers and one gradient copolymer. We find that copolymers with larger width of gradient composition have a broader comonomer distribution along the interface normal, which drastically displaces the immiscible homopolymers from the interface, and hence more pronouncedly enlarges the interfacial thickness and more substantially reduces the interfacial tension. Furthermore, the counteraction effect, which arises from the tendency of heterogeneous segments in gradient copolymers to phase separate and enter their miscible phases to reduce the local enthalpy, reduces the stretching of copolymers along the interface normal direction. Therefore, with the increase of copolymer gradient width, the stretching of copolymer conformations along the interface normal direction is decreased, but the expanding of chain conformations in the plane parallel to the interface is increased. Such conformation changes could yield relatively strong lateral repulsions between copolymers, so that the near-zero interfacial tension is achieved with small volume fraction of copolymers as the copolymer gradient width is increased. For the copolymers with a smaller gradient width, due to the weakening counteraction effect, they have a high degree of orientation ordering at the interface, which enhances their rigidity against bending deformations. Thus, copolymers with a larger width of gradient composition can occupy a larger interfacial area and form softer monolayers at saturation. Therefore, copolymers with a gradient in composition are more efficient in facilitating the formation of microemulsions than traditional diblock copolymers.

Additionally, similar to diblock copolymers, the interfacial properties of gradient copolymers can be altered by the chain length ratio, the segregation strength ε_{AB} of the blend, and the interactions between homopolymers and copolymers. Our simulation studies show that there exists a strong coupling between the comonomer sequence distribution, chain conformation, and interfacial properties. Especially, bending modulus is mainly determined by the complicated interplay of interfacial copolymer density and interfacial chain conformation. For a small chain length ratio, stretching of copolymer conformation along the interface normal is enhanced but the interfacial copolymer density is reduced due to the swelling effect of homopolymers to the copolymer brushes at interface, and thus the bending modulus is insensitive to the variation of the chain length ratio. With increasing segregation strength, copolymers could stretch their conformations along the interface normal and the interfacial copolymer density increases. Thus, bending modulus definitely increases with the segregation strength for diblock copolymers. But for gradient copolymers, the growing tendency of bending modulus with segregation strength becomes weak and bending modulus finally levels off for the copolymers with a wider gradient composition at higher ε_{AB}, as the counteraction effect is significantly enhanced in such cases. Furthermore, increasing the attractions (or decreasing the repulsions) between homopolymers and copolymer chains could increase the saturated area per copolymer due to the enhanced swelling of homopolymers to the copolymer brushes. Meanwhile, the orientation and the stretching of copolymer chains along the interface normal direction are increased with the attractions, and thus the bending modulus of interfacial monolayer increases as well.

dx.doi.org/10.1021/jp3020172 | J. Phys. Chem. B 2012, 116, 9512−9522

All these results demonstrate that the interfacial properties depend significantly on the comonomer sequence distribution of the individual copolymer and chain conformation. The "counteraction effect" of gradient copolymers, which disrupts the stretching and orientation of the interfacial copolymers, always brings a lower bending modulus and a higher interfacial area. Additionally, our previous investigation[36] showed that, as a result of the counteraction effect, the gradient lamellar phase is formed at a higher value of segregation strength, has a shorter periodic length and lower orientational order, and occupies a smaller phase region on the phase diagram. Also, the counteraction effect enhances the conformational entropy loss of homopolymers if located within gradient lamellae and shorter homopolymers are required to form bicontinuous microemulsions. Thus, a fundamental understanding of the comonomer sequence distribution on the interfacial properties and phase behavior of blends with two homopolymers and a gradient copolymer is of great utility in rational selection and design of the comonomer sequence distributions to facilitate the formation of bicontinuous microemulsions.

■ ASSOCIATED CONTENT

Supporting Information

Plots for the phase diagram of a typical ternary blend system and fluctuation spectra of the copolymer monolayers between coexisting homopolymer phases at different box sizes. This material is available free of charge via the Internet at http://pubs.acs.org.

■ AUTHOR INFORMATION

Corresponding Author

*E-mail: hxguo@iccas.ac.cn.

Notes

The authors declare no competing financial interest.

■ ACKNOWLEDGMENTS

This work was supported by the National Natural Science Foundation of China under Grant 20874110 and 21174154.

■ REFERENCES

(1) Morkved, T. L.; Stepanek, P.; Krishnan, K.; Bates, F. S.; Lodge, T. P. *J. Chem. Phys.* **2001**, *114*, 7247.
(2) Morkved, T. L.; Chapman, B. R.; Bates, F. S.; Lodge, T. P.; Stepanek, P.; Almdal, K. *Faraday Discuss.* **1999**, *112*, 335.
(3) Zhou, N.; Lodge, T. P.; Bates, F. S. *J. Phys. Chem. B* **2006**, *110*, 3979.
(4) Nedoma, A. J.; Lai, P.; Jackson, A.; Robertson, M. L.; Balsara, N. P. *Macromolecules* **2010**, *43*, 7852.
(5) Nedoma, A. J.; Lai, P.; Jackson, A.; Robertson, M. L.; Wanakule, N. S.; Balsara, N. P. *Macromolecules* **2010**, *43*, 3549.
(6) Brown, H. R.; Char, K.; Deline, V. R.; Green, P. F. *Macromolecules* **1993**, *26*, 4155.
(7) Lu, J. R.; Li, Z. X.; Su, T. J.; Thomas, R. K.; Penfold, J. *Langmuir* **1993**, *9*, 2408.
(8) Sottmann, T.; Strey, R.; Chen, S.-H. *J. Chem. Phys.* **1997**, *106*, 6483.
(9) Zhou, N.; Bates, F. S.; Lodge, T. P. *Nano Lett.* **2006**, *6*, 2354.
(10) Jones, B. H.; Lodge, T. P. *Chem. Mater.* **2010**, *22*, 1279.
(11) Jones, B. H.; Lodge, T. P. *J. Am. Chem. Soc.* **2009**, *131*, 1676.
(12) Thompson, R. B.; Matsen, M. W. *J. Chem. Phys.* **2000**, *112*, 6863.
(13) Barneveld, P. A.; Hesselink, D. E.; Leermakers, F. A. M.; Lyklema, J.; Scheutjens, J. M. H. M. *Langmuir* **1994**, *10*, 1084.
(14) Müller, M.; Schick, M. *J. Chem. Phys.* **1996**, *105*, 8885.
(15) Lindahl, E.; Edholm, O. *Biophys. J.* **2000**, *79*, 426.
(16) Rekvig, L.; Hafskjold, B.; Smit, B. *J. Chem. Phys.* **2004**, *120*, 4897.
(17) Noolandi, J.; Hong, K. M. *Macromolecules* **1982**, *15*, 482.
(18) Matsen, M. W.; Schick, M. *Macromolecules* **1993**, *26*, 3878.
(19) Thompson, R. B.; Matsen, M. W. *Phys. Rev. Lett.* **2000**, *85*, 670.
(20) Chun, S. B.; Han, C. D. *Macromolecules* **1999**, *32*, 4030.
(21) Kim, H. C.; Nam, K. H.; Jo, W. H. *Polymer* **1993**, *34*, 4043.
(22) Jo, W. H.; Jo, B. C.; Cho, J. C. *J. Polym. Sci, Polym. Phys. Ed.* **1994**, *32*, 1661.
(23) Jo, W. H.; Kim, H. C.; Baik, D. H. *Macromolecules* **1991**, *24*, 2231.
(24) Auschra, C.; Stadler, R.; Voigt-Martin, I. G. *Polymer* **1993**, *34*, 2085.
(25) Fredrickson, G. H.; Bates, F. S. *Eur. Phys. J. B* **1998**, *1*, 71.
(26) Harrats, C.; Blacher, S.; Fayt, R.; Jerome, R.; Teyssie, Ph. *J. Polym. Sci., Part B: Polym. Phys.* **1995**, *33*, 801.
(27) Fleury, G.; Bates, F. S. *Soft Matter* **2010**, *6*, 2751.
(28) Mok, M. M.; Kim, J.; Torkelson, J. M. *J. Polym. Sci., Part B: Polym. Phys.* **2008**, *46*, 48.
(29) Kim, J.; Sandoval, R. W.; Dettmer, C. M.; Nguyen, S. T.; Torkelson, J. M. *Polymer* **2008**, *49*, 2686.
(30) Pakula, T.; Matyjaszewski, K. *Macromol. Theory Simul.* **1996**, *5*, 987.
(31) Shull, K. R. *Macromolecules* **2002**, *35*, 8631.
(32) Kim, J.; Gray, M. K.; Zhou, H.; Nguyen, S. T.; Torkelson, J. M. *Macromolecules* **2005**, *38*, 1037.
(33) Sun, X.; Luo, Y.; Wang, R.; Li, B.; Zhu, S. *AIChE J.* **2008**, *54*, 1073.
(34) Yuan, W.; Mok, M. M.; Kim, J.; Wong, C. L. H.; Dettmer, C. M.; Nguyen, S. T.; Torkelson, J. M.; Shull, K. R. *Langmuir* **2010**, *26*, 3261.
(35) Lefebvre, M. D.; Dettmer, C. M.; McSwain, R. L.; Xu, C.; Davila, J. R.; Composto, R. J.; Nguyen, S. T.; Shull, K. R. *Macromolecules* **2005**, *38*, 10494.
(36) Sun, D.; Guo, H. *Polymer* **2011**, *52*, 5922.
(37) Jiang, R.; Jin, Q.; Li, B.; Ding, D.; Wickham, R. A.; Shi, A. *Macromolecules* **2008**, *41*, 5457.
(38) Ji, S.; Ding, J. *Langmuir* **2006**, *22*, 553.
(39) Yang, Z.; Pan, Z.; Zhang, L.; Liang, H. *Polymer* **2010**, *51*, 2795.
(40) Sariban, A.; Binder, K. *J. Chem. Phys.* **1987**, *86*, 5859.
(41) Metropolis, N.; Rosenbluth, A. W.; Rosenbluth, M. N.; Teller, A. H.; Teller, E. *J. Chem. Phys.* **1953**, *21*, 1087.
(42) Dadmun, M. *Macromolecules* **1996**, *29*, 3868.
(43) Podgornik, R. J. *Stat. Phys.* **1995**, *78*, 1175.
(44) Shi, W.; Guo, H. *J. Phys. Chem. B* **2010**, *114*, 6365.
(45) Laradji, M.; Mouritsen, O. G. *J. Chem. Phys.* **2000**, *112*, 8621.
(46) Laradji, M.; Desai, R. C. *J. Chem. Phys.* **1998**, *108*, 4662.
(47) Shull, K. R.; Kramer, E. J. *Macromolecules* **1990**, *23*, 4769.
(48) Yeung, C.; Shi, A.-C. *Macromolecules* **1999**, *32*, 3637.
(49) Shull, K. R.; Mayes, A. M.; Russell, T. P. *Macromolecules* **1993**, *26*, 3929.
(50) Weyersberg, A.; Vilgis, T. A. *Phys. Rev. E* **1993**, *48*, 377.
(51) Larson, R. G. *J. Chem. Phys.* **1989**, *91*, 2479.
(52) Noolandi, J.; Hong, K. M. *Macromolecules* **1984**, *17*, 1531.
(53) Anastasiadis, S. H.; Gancarz, I.; Koberstein, J. T. *Macromolecules* **1989**, *22*, 1449.
(54) Retsos, H.; Margiolaki, I.; Messaritaki, A.; Anastasiadis, S. H. *Macromolecules* **2001**, *34*, 5295.
(55) Wang, R.; Li, W.; Luo, Y.; Li, B.; Shi, A.; Zhu, S. *Macromolecules* **2009**, *42*, 2275.
(56) Szleifer, I.; Kramer, D.; Ben-Shaul, A.; Gelbart, W. M.; Safran, S. A. *J. Chem. Phys.* **1990**, *92*, 6800.
(57) Szleifer, I.; Kramer, D.; Ben-Shaul, A.; Roux, D.; Gelbart, W. M. *Phys. Rev. Lett.* **1998**, *60*, 1966.
(58) Marrink, S. J.; Mark, A. E. *J. Phys. Chem. B* **2001**, *105*, 6122.
(59) Würger, A. *Phys. Rev. Lett.* **2000**, *85*, 337.
(60) Matsen, M. W. *J. Chem. Phys.* **1999**, *110*, 4658.

(61) Rosen, M. J.; Cohen, A. W.; Dahanayake, M.; Hua, X. *J. Phys. Chem.* **1982**, *86*, 541.
(62) Chun, S. B.; Han, C. D. *Macromolecules* **2000**, *33*, 3409.